

RELIABILITY-BASED INSPECTION SCHEDULE FOR DAMAGE-TOLERANT STRUCTURES

Hiroo ASADA, Seiichi ITO and Hirokazu SHOUJI

Airframe Division
National Aerospace Laboratory
Tokyo, Japan

Yasuhiro TOI, Yasuhiro FUJIWARA, Takaharu OYAGI and Junji TAKAKI

Aerospace Division
Fuji Heavy Industries, Ltd
Utsunomiya, Japan

1. INTRODUCTION

Adequate inspection schedules are considered to play increasingly an important role in maintaining the structural integrity of advanced aircraft designed by the damage-tolerant method¹⁻⁴⁾. A rational determination of inspection schedules, sample size, first inspection time and inspection intervals is the key to effective detection, repair and replacement of fatigue cracks, and the resulting failed elements in order to maintain the required reliability of aircraft structures. Structural reliability analysis is realized to be a useful tool⁴⁾ for developing adequate inspection schedules because several primary factors, such as initial crack length, fatigue crack initiation time, fatigue crack propagation, service loads, residual strength, and crack detection capability, are probabilistic and need to be treated in the analysis.

For the reliability analysis to be performed with a high degree of engineering soundness, the probabilistic models used for the analysis must be defined reasonably well. However, the usual paucity of pertinent data makes it difficult for the probability density functions of those factors and of their respective parameter values to be determined. Although actual data collected during in-service inspections is limited in quantity as well as quality, it is a valuable source of highly useful information that will be utilized not only to determine reliability-based inspection schedules but also to estimate uncertain parameters in the physical model.

From this point of view, this research concentrates on the development of Bayesian reliability analysis⁵⁻⁸⁾, which can estimate subjectively appropriate values of uncertain parameters with decision-making on the basis of posterior probability and can develop optimal non-periodic inspection schedules utilizing small sample field data collected during inspections.

A fatigue-critical element model used in the present study is a two-bay fail-safe structure in the fuselage which consists of multiple components, namely, three frames and a skin panel. This element is subjected to cyclic stress due to differential pressure and is designed in accordance with the damage-tolerant method. Monte Carlo simulations are carried out to generate the failure process in the structural element and to demonstrate the validity of the proposed Bayesian reliability methodology.

2. FATIGUE-CRITICAL STRUCTURAL ELEMENT MODEL

2.1 True Element Model

For a fatigue-critical structural element in Figure 1, the materials of skin and frames are 2024-T3 and 7075-T6 aluminum alloys, respectively. The failure process consists of crack initiation, propagation and unstable crack growth. Fatigue cracks in the element propagate to the longitudinal direction of fuselage.

1) Applied load

Aircraft fuselage structures are subjected to several kinds of loads. In this analysis, however, it is

considered that the structural element is only subjected to cyclic constant stress Δs due to the cabin differential pressure for each flight. This stress depends on a location of the element, and Δs is assumed to be a random variable normally distributed.

2) Fatigue crack initiation

Fatigue cracks initiate simultaneously at both sides of rivet holes in the skin and the center frame. The initial half crack length a_0 is assumed to be the sum of the hole radius r_0 and the initial through crack length a_i shown in Figure 2. The time to crack initiation (TTCI) t_0 is a random variable governed by a two-parameter Weibull distribution:

$$f_0(t_0) = \frac{\alpha}{\beta} \left(\frac{t_0}{\beta}\right)^{\alpha-1} \exp\left\{-\left(\frac{t_0}{\beta}\right)^\alpha\right\} \quad (1)$$

3) Fatigue crack propagation

Fatigue cracks on both sides of the rivet holes of a skin plate a_s and a center frame a_f subjected to cyclic loading propagate under the Paris law with the stress intensity factor range modified by coefficients β :

$$(1) \text{ Skin } a_s: \quad \frac{da_s}{dt} = C_S (\Delta K_S)^{b_S} \quad (2)$$

$$\left. \begin{aligned} \Delta K_S &= \Delta s \sqrt{\pi a_s} \beta_{\text{Frame}} \beta_{\text{Bulge}} \\ C_S &= 10^{z_S} \end{aligned} \right\} \quad (3)$$

$$(2) \text{ Frame } a_f: \quad \frac{da_f}{dt} = C_F (\Delta K_F)^{b_F} \quad (4)$$

$$\left. \begin{aligned} \Delta K_F &= \Delta s \sqrt{\pi a_f} \beta_{\text{WF}} \beta_{\text{Skin}} \\ C_F &= 10^{z_F} \end{aligned} \right\} \quad (5)$$

in which parameters z_s and z_f are random variables assumed to be normally distributed. The period of skin fatigue crack propagation lies between t_0 and t_f shown in Figures 2 and 3. During that period, the crack propagates from a_0 to a_f . The variables, t_f and a_f , denote the time and the crack length when the element fails as mentioned below.

4) Element failure criterion

An element can fail either before or after fatigue crack initiation. Before crack initiation, the element is considered to have failed when the stress due to differential pressure exceeds the strength of the element. After crack initiation, the following two failure modes are considered to exist. A failure due to unstable crack growth occurs when the crack length reaches a certain level a_f which is derived by a failure criterion. This unstable crack is arrested at both sides of frames because the residual strength increases near the frames. The other failure mode arises when a fatigue crack reaches the 2-bay fail-safe crack length which is equivalent to a_f . Feddersen's criterion of residual strength is adopted for the condition of unstable crack propagating. This criterion involves yield stress S_y and fracture toughness K_{Ic} , both of which are random variables governed by two-parameter Weibull distributions.

2.2 Element Model for Bayesian Reliability Analysis

External detailed visual inspection is implemented in order to detect skin cracks in the element

shown in Figure 1. Therefore, a skin crack a_s is only used in the analysis. As shown in Figures 2 and 3, a_s is visually detectable when it exceeds $a_0^* = r_h + a_{min}$. The variables r_h and a_{min} denote the rivet head radius and the minimum detectable crack length due to visual inspection respectively. The detectable crack propagation period lies between t_0^* and t_f . The TTCI of this model t_0^* is much longer than that for the true model t_0 .

1) Fatigue crack initiation

The TTCI of the model is assumed to be a random variable with the density function of a two-parameter Weibull distribution:

$$f_0^*(t_0^*|\beta^*) = \frac{\alpha}{\beta^*} \left(\frac{t_0^*}{\beta^*}\right)^{\alpha-1} \exp\left\{-\left(\frac{t_0^*}{\beta^*}\right)^\alpha\right\} \quad (6)$$

Uncertainty is introduced in the TTCI through the scale parameter β^* which is a random variable.

2) Fatigue crack propagation

The period of skin fatigue crack propagation is defined between t_0^* and t_f when the element fails. During that period, the crack propagates from a_0^* to a_f . The following Paris equation is used to present a skin fatigue crack propagation:

$$\frac{da_s}{dt} = C(a_s)^{b/2} \quad (7)$$

$$C = 10^z$$

Integrating Eq.(7) from a_0^* to the current crack length a_s at time t , the following expression is obtained:

$$a_s(t-t_0^*|z) = \{-b'10^z(t-t_0^*)-a_0^{*b'}\}^{-1/b'} \quad (8)$$

$$b' = (b-2)/2$$

$$a_0^* = r_h + a_{min}$$

Uncertainty in fatigue crack propagation is introduced by a random variable z .

3) Inspection

All structural elements are inspected by external detailed visual inspection at the time of each inspection. It is assumed that element failure can be detected always if it exists during the inspection process. Therefore, the probability of detecting the element failure is equal to unity.

4) Probability of crack detection for visual inspection

Information on the probabilities of crack detection (POD) is necessary in the present analysis.

(1) Probability of detection for a crack

The probability that a crack will be detected, $D(a_s^*|d)$, by visual inspection depends on the crack size in excess of the radius r_h of the rivet head shown in Figure 2 and is assumed to be given by a three-parameter Weibull function as shown below:

$$D(a_s^*|d) = 1 - \exp\left\{-\left(\frac{a_s^* - a_{min}}{d - a_{min}}\right)^\epsilon\right\} \quad (9)$$

Then, the probability that the crack will not be detected is given by:

$$\bar{D}(a_s^*|d) = 1 - D(a_s^*|d) \quad (10)$$

where $a_s^* = a_s - r_h$ and a_{\min} denote the inspectable and the minimum detectable crack length.

(2) Probability of detection for cracks at a rivet

Both sides of the rivet head are inspected for cracks. As it is assumed that the skin crack is always symmetric about the central axis, the probability $D_t(a_s^*|d)$ that at least the crack on the one side is detected is given by:

$$D_t(a_s^*|d) = 1 - \bar{D}_t(a_s^*|d) \quad (11)$$

where $\bar{D}_t(a_s^*|d)$ is:

$$\bar{D}_t(a_s^*|d) = [\bar{D}(a_s^*|d)]^2 \quad (12)$$

5) Repair or replacement

If a crack is detected in the skin of the element, the skin and frame are repaired or replaced and the element regains its initial strength.

6) Failure rate and element reliability

Based on the element failure criterion, following two failure rates are defined.

(1) Before crack initiation

The failure rate at time instant t before crack initiation is a very small constant and given by:

$$\text{Failure rate:} \quad h(t) = \exp(r) = h_0 \quad (13)$$

$$\text{Reliability:} \quad U(t-T_i) = \exp\left\{-\int_0^{t-T_i} h(\tau) d\tau\right\} = \exp\{-(t-T_i) \cdot \exp(r)\} \quad (14)$$

(2) After crack initiation

A two-parameter Weibull function is adopted for the failure rate after crack initiation at time instant t :

$$\text{Failure rate:} \quad h(t) = \frac{\alpha_f}{\beta_f} \left(\frac{t}{\beta_f}\right)^{\alpha_f - 1} + \exp(r) \quad (15)$$

Reliability:

$$V(t-t_0^*) = \exp\left\{-\int_0^{t-t_0^*} h(\tau) d\tau\right\} = \exp\left\{-\frac{1}{\beta_f^{\alpha_f}} (t-t_0^*)^{\alpha_f} - (t-t_0^*) \exp(r)\right\} \quad (16)$$

7) Uncertain parameters

Two parameters β^* and z are estimated from inspection data such as the number of cracks, crack sizes and whether or not failures were observed. Other parameters are assumed to be known.

3. FORMULATION OF BAYESIAN RELIABILITY ANALYSIS

3.1 Possible Events at Time of Inspection

At the time of the j -th inspection performed at time T_j on a certain element, one of the following

five events may occur (knowing that this element was repaired or replaced during the l -th inspection performed at time T_l with $l < j$):

- 1) { $A: j, l$ } : event that the element is found to have failed at the time of the j -th inspection T_j . This event consists of the following two mutually exclusive events:
 - [1] E_{1j} : event that the element failed before crack initiation, sometime during the time interval $[T_{j-1}, T_j]$.
 - [2] E_{2j} : event that the element failed after crack initiation, sometime during the time interval $[T_{j-1}, T_j]$.
- 2) { $B_1(a_j): j, l$ } : event that a crack of length between a_j and a_j+da_j is detected in the element : E_{3j} .
- 3) { $B_2: j, l$ } : event that no crack is detected in the element. This event consists of the following two mutually exclusive events:
 - [1] E_{4j} : event that the element did not fail in the time interval $[T_{j-1}, T_j]$ and no crack exists in the element at the time of inspection T_j .
 - [2] E_{5j} : event that the element did not fail in the time interval $[T_{j-1}, T_j]$ but a crack exists in the element which is not detect at the time of inspection T_j .

The probabilities of these five events will be evaluated for a particular element in terms of the probability density and distribution functions $f_0^*(t|\beta^*)$ and $F_0^*(t|\beta^*)$ of the TTCL, a skin crack a_s , reliability functions $U(t)$ and $V(t)$ and probability of crack detection $D_t(a|d)$.

3.2 Reliability of an Element After the Latest Inspection T_j

The reliability of two types of elements at time instant t^* after the j -th inspection is calculated in the following:

- 1) Elements repaired or replaced at the j -th inspection

Elements are repaired or replaced at the j -th inspection in the case of events { $A: j, l$ } or { $B_1(a_j): j, l$ }, respectively:

Reliability:

$$R(t^*; \text{Repair}) = \{1 - F_0^*(t^* - T_j | \beta^*)\} \cdot U(t^* - T_j) + \int_{T_j}^{t^*} f_0^*(t - T_j | \beta^*) \cdot U(t - T_j) \cdot V(t^* - t) dt \quad (17)$$

- 2) Elements not Repaired at the j -th Inspection

An element is neither repaired nor replaced at the j -th inspection in the case of event { $B_2: j, l$ }:

Reliability:

$$R(t^*; \text{No Repair}) = \frac{Q}{P\{B_2: j, l\}} \quad (18)$$

$$Q = \{1 - F_0^*(t^* - T_j | \beta^*)\} \cdot U(t^* - T_j) + \int_{T_j}^{t^*} f_0^*(t - T_j | \beta^*) \cdot U(t - T_j) \cdot V(t^* - t) dt + \sum_{i=1}^{j-1} \int_{t_i}^{t_{i+1}} f_0^*(t - T_i | \beta^*) \cdot U(t - T_i) \cdot V(t^* - t) \cdot \left[\prod_{k=i+1}^j [1 - D_t(a_s(T_k - t|z))] \right] dt \quad (19)$$

3.3 Uncertain Parameters by Bayesian Analysis

- 1) Prior joint density function of uncertain parameters

Initially, it is assumed that b^* and z are jointly and uniformly distributed according to the following

prior joint density function:

$$f^0(\beta^*, z) = \frac{1}{(\beta^*_{\max} - \beta^*_{\min})(z_{\max} - z_{\min})} \quad (20)$$

where:

$$\beta^*_{\min} \leq \beta^* \leq \beta^*_{\max}; \quad z_{\min} \leq z \leq z_{\max} \quad (21)$$

2) Likelihood function resulting from j-th inspection

The likelihood function LF_j for the entire structure as a result of the j-th inspection is calculated as:

$$LF_j = \prod_{m=1}^M LF_j^{(m)} \quad (22)$$

where $LF_j^{(m)}$ is the likelihood function for element m resulting from the j-th inspection and M is the total number of elements in the structure.

3) Posterior joint density function of uncertain parameters

The posterior joint density function of the two uncertain parameters β^* and z immediately after the j-th inspection, is given by:

$$f^j(\beta^*, z) = \frac{LF_j \cdot f^0}{\int_{\beta^*_{\min}}^{\beta^*_{\max}} \int_{z_{\min}}^{z_{\max}} (\text{Numerator}) d\beta^* dz} \quad (23)$$

3.4 Reliability of Entire Structure at Time Instant t^* After the Latest Inspection T_j

The reliability of the entire structure consisting of M elements at time instant t^* after the latest inspection T_j is denoted by $\bar{R}_M(t^*)$ and calculated as:

$$\bar{R}_M(t^*) = \int_{\beta^*_{\min}}^{\beta^*_{\max}} \int_{z_{\min}}^{z_{\max}} R_M(t^* | \beta^*, z) \cdot f^j(\beta^*, z) d\beta^* dz \quad (24)$$

where:

$$R_M(t^* | \beta^*, z) = \left[\prod_{m=1}^{M_1} R_m(t^*; \text{Repair}) \right] \cdot \left[\prod_{m=1}^{M_2} R_m(t^*; \text{No Repair}) \right] \quad (25)$$

where M_1 is a number of elements either repaired or replaced at the j-th inspection, M_2 is a number of elements found intact at the j-th inspection and $M_1 + M_2 = M$. In Eq.(25), $R_m(t^*; \text{Repair})$ and $R_m(t^*; \text{No Repair})$ are identical with the reliabilities $R(t^*; \text{Repair})$ and $R(t^*; \text{No Repair})$ defined in Eqs.(17) and (18), respectively. Note that $R_m(t^*; \text{Repair})$ and $R_m(t^*; \text{No Repair})$ are conditional to given values of β^* and z .

3.5 Calculation of Time T_{j+1} for Next Inspection

Assuming that the entire structure must maintain its reliability above a prespecified design level throughout its service life, the time T_{j+1} for the next inspection after the latest one performed at T_j is calculated using:

$$\bar{R}_M(t^*) \geq R_{\text{design}} \quad (26)$$

where R_{design} denotes the prespecified design level of reliability for the entire structure. The time T_{j+1} of

the (j+1)-th inspection is then estimated as the maximum value of t^* that satisfies Eq.(26) as follows:

$$T_{j+1} = t^* = \bar{R}_M^{-1}(R_{design}) \quad (27)$$

It is obvious that the reliability of the entire structure remains above the prespecified design level R_{design} , through- out the service life of the structure.

4. NUMERICAL EXAMPLE

All the values of a true structural element model and a Bayesian analysis model listed in Table 1 are approximately corresponding to these applicable to an actual fuselage structural design. Monte Carlo simulations are performed to generate the failure process in the true structural element.

Two essential uncertain parameters β^* and z are set to be jointly and uniformly distributed according to the following initial prior joint density function shown by Eq.(20). The minimum and maximum values of these parameters, and their ranges and increments are given by the engineering judgment as follows:

$$\beta^*_{min} = 17,000 \text{ flights} ; \quad \beta^*_{max} = 66,000 \text{ flights} ; \quad \bar{\beta}^* = \beta^*_{max} - \beta^*_{min} = 49,000 \text{ flights}; \\ \Delta\beta^* = 3,500 \text{ flights}$$

$$z_{min} = -4.1 ; \quad z_{max} = -2.7 ; \quad \bar{z} = z_{max} - z_{min} = 1.4; \quad \Delta z = 0.1$$

The aircraft is assumed to have 100 or 200 fatigue-critical elements. The service life is 50,000 flights and the minimum reliability level for the entire structure throughout its service life is set equal to $R_{design} = 0.8$. This indicates that the reliabilities of one element for both 100 and 200 fatigue-critical elements are 0.998 and 0.999, respectively under the assumption of independence. The standard deviation σ_z of z for the parameters of fatigue crack propagations of skin and frame in Eqs.(2) to (5) is set at 0.154. This indicates that the speeds of fatigue crack propagation between twice and half the mean crack propagation speeds of skin and frame account for 95% of all fatigue cracks. The values of the parameters ϵ and a_{min} in the POD of Eq.(9) are given as $\epsilon = 1.4$ and $a_{min} = 0.04$ inches based on the field data⁹ of fatigue cracks visually detected. A parametric study on the parameter d in the POD is performed for $d = (1.2, 1.4, 1.6, 1.8)$ inches, in order to investigate its effect on crack detection capability.

The reliability curves of the entire structure as a function of time for each combination of $M = (100, 200)$ and $d = (1.2, 1.4, 1.6, 1.8)$ inches are depicted in Figures 4 and 5 with numbers of failed elements and of detected cracks. It is shown that the inspections are implemented non-periodically. The reliability returns to the unity after inspections and decreases along operation. The following inspection is implemented at the reliability equal to $R_{design} = 0.8$ and shorter inspection intervals are given with the progress of operation. The first inspection times T_1 for $M = (100, 200)$ and $d = (1.2, 1.4, 1.6, 1.8)$ inches are performed after approximately 30,000 flights due to the ranges of the parameter values, β^* and z , introduced by the engineering judgment in this analysis. In the case that the number of critical elements increases, the number of inspections during service life for each parameter d in the POD increases in order to maintain the same target reliability R_{design} , and the numbers of failed elements and detected cracks also increase. When the value of the parameter d in the POD gets larger, namely the crack detection becomes less efficient, the number of inspections increases, and the inspection intervals become shorter to keep the minimum level of reliability R_{design} for the entire structure. When the number of critical elements and the value of the parameter d become large, several elements would have failed before they were detected by external detailed visual inspection.

The posterior joint density functions of the uncertain parameters, β^* and z , after the third inspection are plotted in Figures 6 and 7 for $M = (100, 200)$ and $d = (1.2, 1.4, 1.6, 1.8)$ inches,

respectively. The concentration of posterior joint density at the modal values for $M = 100$ is sharper than that for $M = 200$, because the number of cracks found at the third inspection for $M = 200$ is smaller than that for $M = 100$. It is anticipated that the concentration is around the reasonable modal value.

5. CONCLUSIONS

The damage tolerant fuselage structure of an aircraft is analyzed and the usefulness of the Bayesian reliability analysis has been demonstrated. The results of the numerical examples verify that this analysis can indeed generate appropriate non-periodic inspection schedules with the estimation of uncertain parameters even if a large number of crack data could not be collected during inspections. If a fleet of aircraft can be inspected as in the actual case, a large number of cracks and possibly failures will be found and it makes the Bayesian analysis even more practical. It is also pointed out that the present study has evaluated the generation of the failure process consisting of fatigue crack initiation and propagation and final failure in the structure element.

ACKNOWLEDGMENTS

The authors are indebted to Professor Masanobu Shinozuka of University of Southern California, Professor Hiroshi Itagaki of Yokohama National University and Professor George Deodatis of Princeton University for their useful suggestion and advice on the Bayesian reliability analysis. They also thank Mr. Tom Swift and Dr. Sam Sampath of the Federal Aviation Administration for their technical assistance and suggestion on the damage-tolerant design.

REFERENCES

- 1) Swift, T. ; Damage Tolerance Capability, *International Journal of Fatigue*, Vol.16, No.1 (1/1994), pp.75-93.
- 2) Swift, T. ; Widespread Fatigue Damage Monitoring -Issues and Concerns, Proceedings of FAA/NASA International Symposium on Advanced Structural Integrity Methods for Airframe Durability and Damage Tolerance, NASA Conference Publication 3274 Part 1 (5/1994), pp.829-870.
- 3) Federal Aviation Administration, FAR 25.571(Draft)(7/1993) ; Damage-Tolerance and Fatigue Evaluation of Structure, and Advisory Circular AC No.25.571-1B(Draft) (7/1993).
- 4) Goranson, U.G. ; Damage Tolerance - Facts and Fiction, Proceedings of the 17th Symposium of the International Committee on Aeronautical Fatigue, ICAF, Vol.1 (6/1993) pp.3-105.
- 5) Asada, H., Itagaki, H. and Ito, S. ; Effect of Sampling Inspections on Aircraft Structural Reliability, Proceedings of ICOSSAR '85, the 4th International Conference on Structural Safety and Reliability, IASSAR Publication, Vol.1 (5/1985) pp.1.87-1.96.
- 6) Deodatis, G., Fujimoto, Y., Ito, S., Spencer, J. and Itagaki, H. ; Non-Periodic Inspection by Bayesian Method I, *Probabilistic Engineering Mechanics J.*, Vol.7, No.4 (1992) pp.191-204.
- 7) Ito, S., Deodatis, G., Fujimoto, Y., Asada, H. and Shinozuka, M. ; Non-Periodic Inspection by Bayesian Method II: Structures with Elements Subjected to Different Stress Levels, *Probabilistic Engineering Mechanics J.*, Vol.7, No.4 (1992) pp.205-215.
- 8) Shinozuka, M., Deodatis, G., Sampath, S. and Asada, H. ; Statistical Property of Widespread Fatigue Damage, AGARD, the 80th Meeting of the Structures and Materials Panel, Specialists' Meeting on Widespread Fatigue Damage in Aircraft (5/1995).
- 9) Endoh, S., Tomita, H., Asada, H. and Sotozaki, T. ; Practical Evaluation of Crack Detection Capability for Visual Inspection in Japan, Proceedings of the 17th Symposium of the International Committee on Aeronautical Fatigue, ICAF, Vol.1 (6/1993) pp.259-280.

Table 1 Values of Parameters in Numerical Example

Item	Values for true model	Bayesian analysis	
		Model value	Range for estimation
·Service life (flights)		50,000	
·Minimum level of reliability	R_{design}	0.8	
·Total number of critical elements	M	100, 200	
·Parameters of TTCI in Eq.(1) 2-parameter Weibull	α	4	4
	β (flights)	40,000	
	β^* (flights)		Unknown
			17,000 to 66,000
·Rivet head radius r_h (in)		0.18	0.18
·Initial half crack length for true model a_0 (in)		0.1	
·Initial half crack length for Bayesian analysis a_0^* (in)			0.22
·Minimum detectable crack length	a_{min} (in)		0.04
·Effective width (in) Skin	W_S	40	
Frame	W_{F1}	14	
	W_{F2}	2	
·Maximum allowable crack length $a_{max}=W/2$ (in) Skin	$a_{S,max}$	20	20
Frame	$a_{F1,max}$	7	
	$a_{F2,max}$	1	
		2024-T3 (Skin:S)	7075-T6 (Frame:F)
·Yield stress S_y (ksi) 2-parameter Weibull	α_{Sy}	19	19
	β_{Sy} (ksi)	49	70
·Fracture toughness K_c (ksi \sqrt{in}) 2-parameter Weibull	α_{Kc}	12	12
	β_{Kc} (ksi \sqrt{in})	140	65
·Fatigue crack propagation in Eqs.(2) & (3) Normal	b	3.8	3.4
	μ_z	-9.5	-9.0
	σ_z	0.154	0.154
in Eq.(5)	b		4.0
	z		Unknown
			-4.1 to -2.7
·Cyclic stress range in Eqs.(2) & (3) Normal	Δs (ksi)		
	$\mu_{\Delta s}$ (ksi)	18	
	$\sigma_{\Delta s}$ (ksi)	0.9	
·Parameters of POD in Eq.(7)	ϵ		1.4
	d (in)	1.2, 1.4, 1.6, 1.8	
·Parameters of failure rate in Eq.(11)	r		-18
in Eq.(13)	α_f		5.5
	β_f (flights)		37,000

Note: 1 ksi=6.895 MPa, 1 in=2.54 cm, 1 ksi \sqrt{in} =1.099 MPa \sqrt{m}

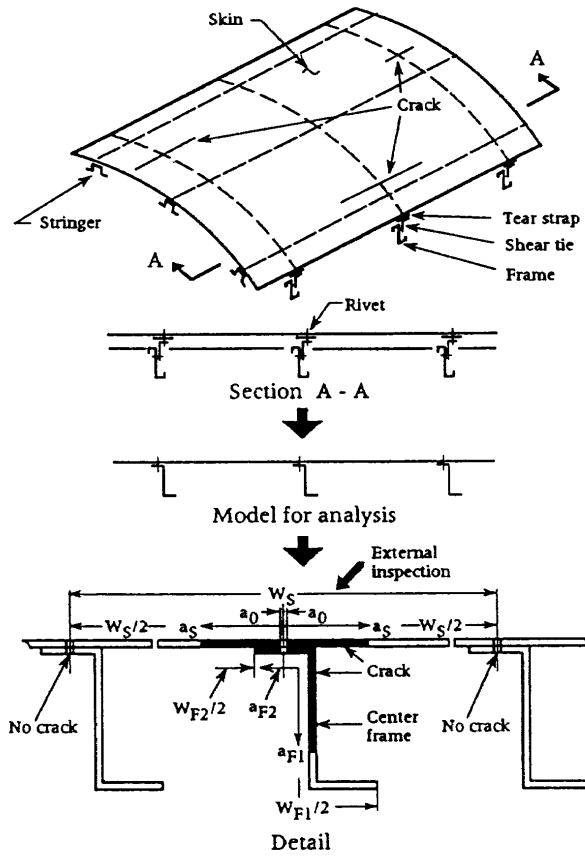


Figure 1 Fuselage Structural Model

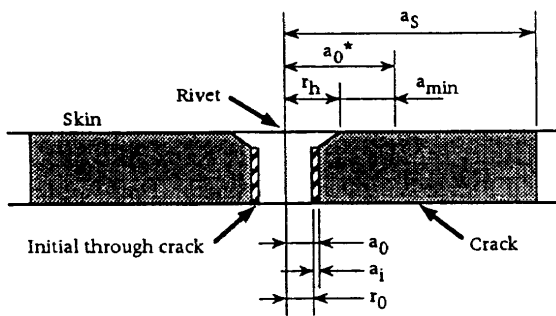


Figure 2 Definition of Rivet and Crack

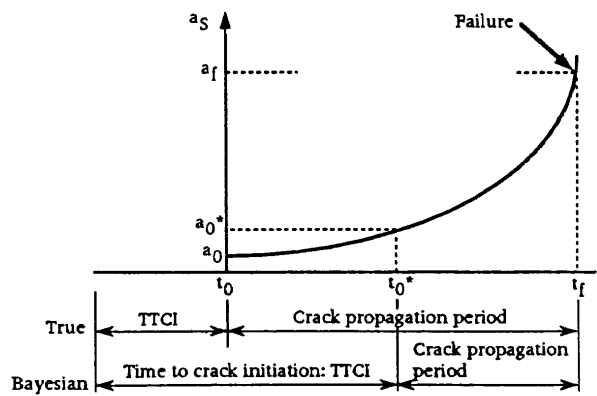


Figure 3 Fatigue Crack Initiation and Propagation for True Model and Bayesian Analysis Model

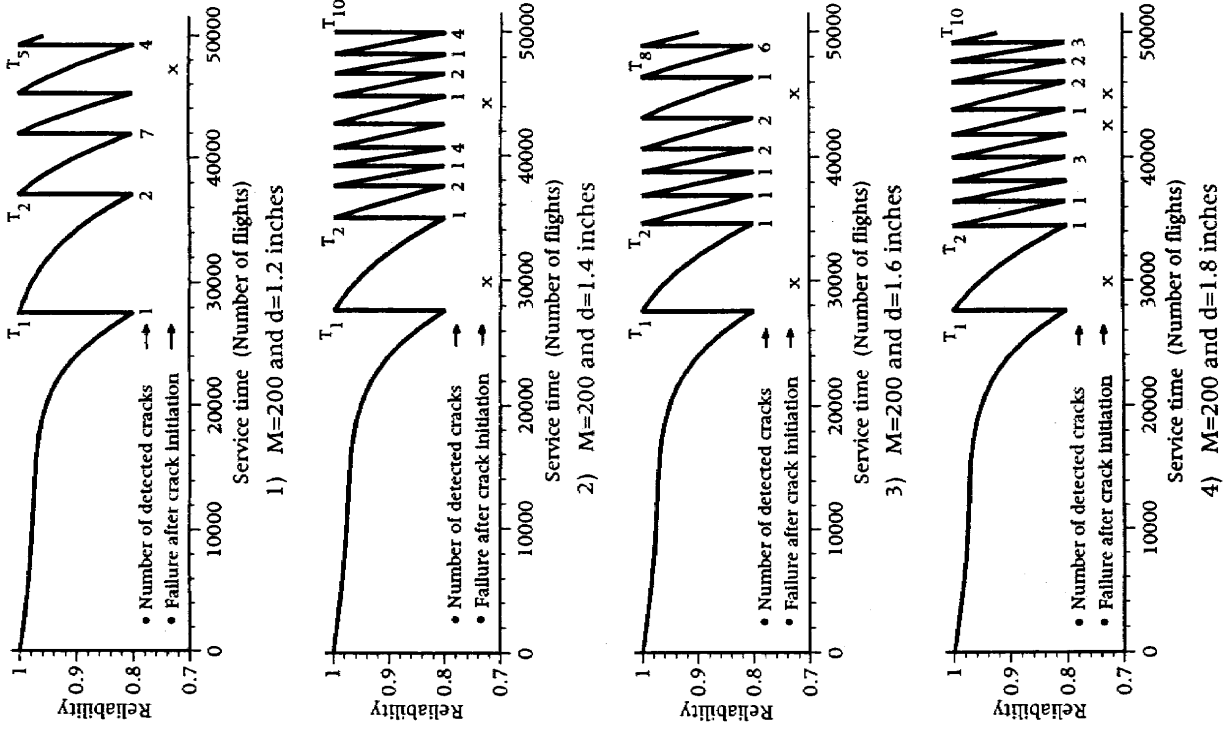


Figure 5 Inspection Schedule and Structural Reliability ($M=200$ and Uncertain Parameters : β^* and z)

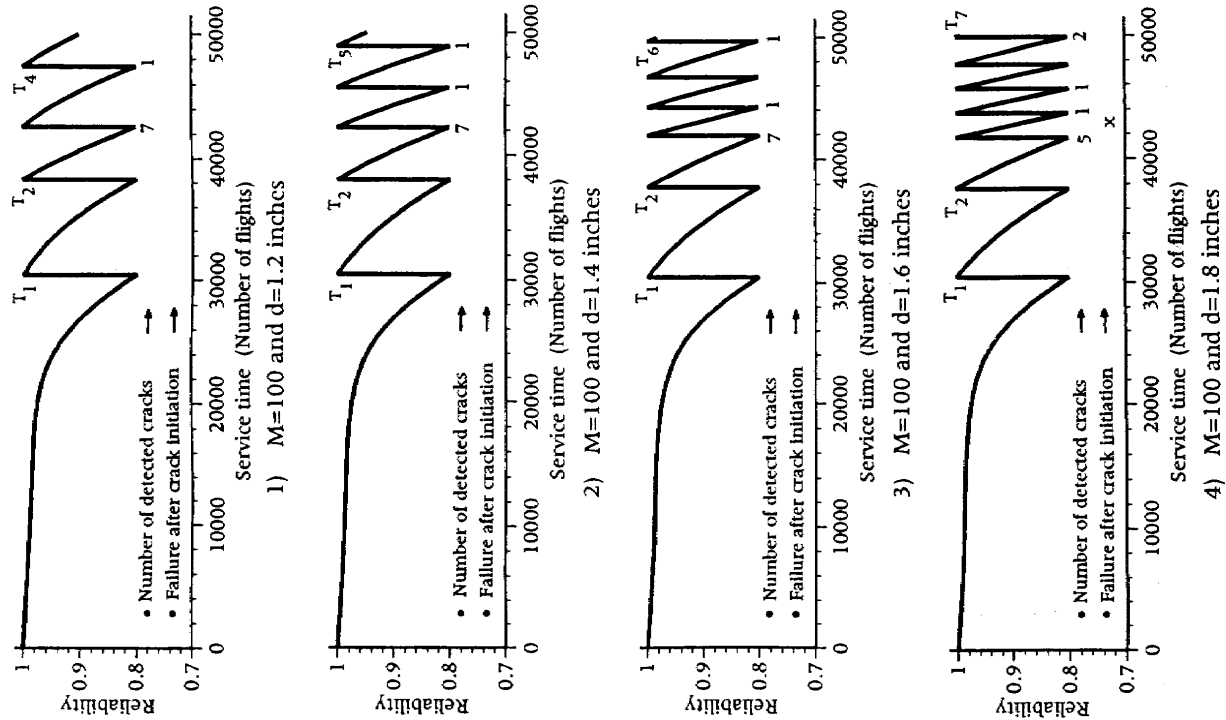
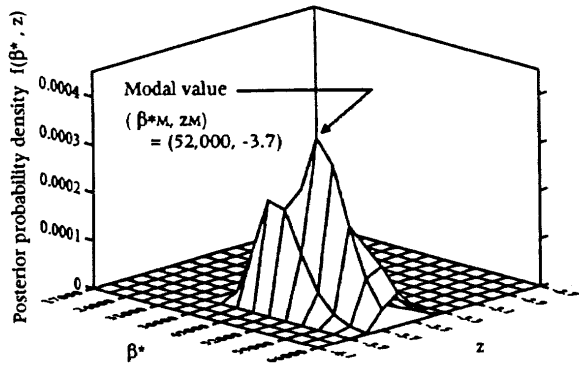
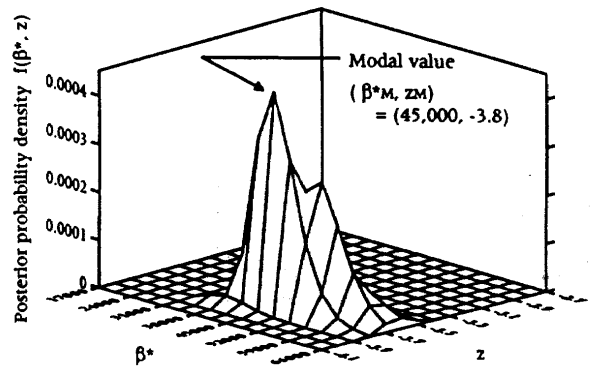


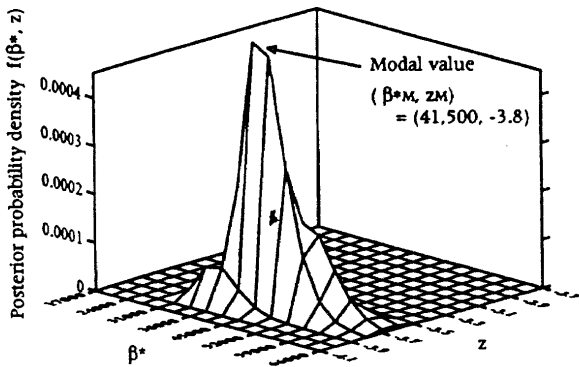
Figure 4 Inspection Schedule and Structural Reliability ($M=100$ and Uncertain Parameters : β^* and z)



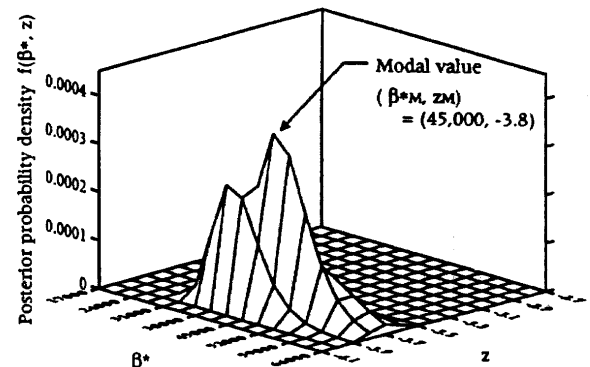
1) M=100 and d=1.2 inches



2) M=100 and d=1.4 inches

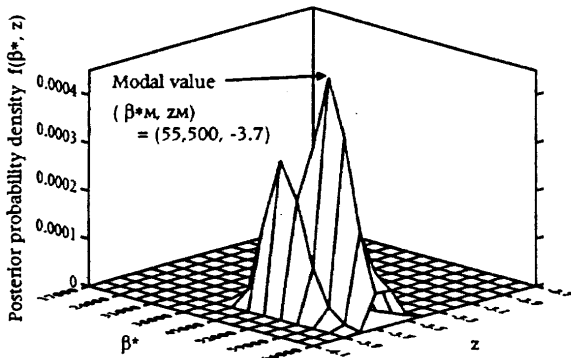


3) M=100 and d=1.6 inches

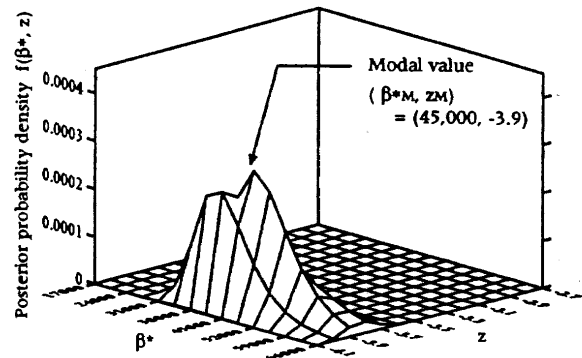


4) M=100 and d=1.8 inches

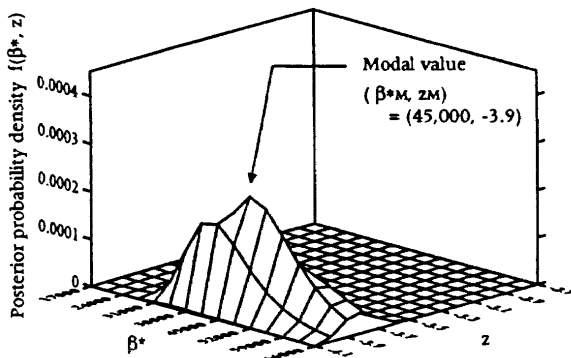
Figure 6 Posterior Joint Probability Density Functions at 3rd Inspection (M=100 and Uncertain Parameters : β^* and z)



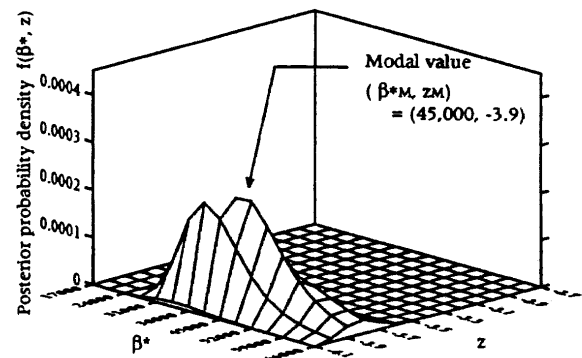
1) M=200 and d=1.2 inches



2) M=200 and d=1.4 inches



3) M=200 and d=1.6 inches



4) M=200 and d=1.8 inches

Figure 7 Posterior Joint Probability Density Functions at 3rd Inspection (M=200 and Uncertain Parameters : β^* and z)